Original scientific paper

Electrochemical studies of lateral flow assay test results for procalcitonin detection

Yachana Gupta, Kalpana, Aditya Sharma Ghrera✉

Applied Science Department, The NorthCap University, Gurugram, India

Corresponding author: ✉*adityasghrera@gmail.com*

Abstract

In this study, the lateral flow assay (LFA) has been developed for the detection of bacterial infection (BI) by specific biomarker procalcitonin (PCT), without a need for complicated instrumentations and technical expertise. For the development of the assay, gold nanoparticles (AuNP) and their conjugates with antibodies specific to the model antigen PCT are assessed. Polyclonal antibody (pAb) labelled with gold nanoparticles (AuNP) to obtain the AuNP-pAb complex and the specific monoclonal antibody (mAb) have been dropped at the test zone. This complex is placed over the conjugate line of the LFA strip. In the absence of PCT or the presence of other biomarkers, the test line remained colourless, which revealed the specificity of assay towards PCT among a pool of various analytes. Herein, observations have been made through two different platforms for quantitative and qualitative analysis for the detection of PCT biomarker. The qualitative analysis has been performed on the basis of appearance red color in the test band, while for quantitative analysis, a novel approach has been adopted. Herein, the nitrocellulose membrane (paper strip) is cut out from the LFA strip and used for electrochemical studies under similar solution conditions. Different paper strips presented different cyclic voltammograms (CV) that could be correlated to varying PCT concentrations captured at the test line of the paper strip. The qualitative detection limit for PCT using this LFA was determined to be 2 ng ml^{-1} and the quantitative detection limit was 1 ng ml^{-1}. The electrochemical response studies of the paper strip by CV technique revealed the sensitivity value of 0.695 μA ml ng^{-1}.

Introduction

Globally, bacterial infections (BI) are one of the primary reasons for illness and death, and they are becoming an increasingly serious problem due to the regular growth of bacteria. According to WHO report, antibiotic-resistant bacteria pose a risk to public health. Therefore, for BI's diagnosis and

immediate response, some on-site detection technique is required [1]. For the clinical utility of BI specific biomarkers, numerous immunoassays like time-resolved fluoro-immunoassay (TRFIA) [2,3], chemi-luminescence immunoassays (CLIA) [4], immunochromatographic tests (ICT), and enzyme-linked immunosorbent assays (ELISA) [5] have been presented in a wide variety of research applications for diagnosis purposes. Nevertheless, the lateral flow immunoassay (LFA) remains an ideal technique for the point of care (POC) testing of BI and any other pathological changes inside the human body [6]. LFA technique allows even unskilled users to perform difficult tests at the point of need in a cost-effective manner and without the need for any additional equipment, which makes it popular among users. As a labeling agent, gold nanoparticles (AuNP) [7] remain of interest to date for LFA development, owing to their enriched intensity, optical stability, biocompatibility, and easy surface modification properties [8,9]. In several already reported studies [10,11], the LFA technique was used to detect BI-specific biomarker procalcitonin (PCT) by AuNP as a label. For the diagnosis of BI or sepsis, PCT acts as a forerunner of the hormone calcitonin and can differentiate between bacterial and viral infections [10,12]. In serum, the value of PCT is < 0.1 ng ml^{-1}, which rises with the severity of the infection. During BI in healthy adults, PCT is < 0.05 µg ml^{-1}, if the systemic infection is unlikely. In the case of localized infection, PCT increases from 0.05 to <0.5 µg ml^{-1}, while in the conditions like major trauma, recent surgery, or severe cardiogenic shock, PCT rises further from 0.5 to <2 µg ml^{-1} [13-15].

Some reported works have developed LFA strips using spherical and popcorn-like AuNP to detect varying PCT concentrations on multiple test lines [16-18]. In the present work, procalcitonin (PCT) has been selected for BI diagnosis as a model antigen taken from the literature [19]. Regarding the new approach to PCT detection, the results of the test line of LFA strips were examined by qualitative and quantitative determinations. Test line qualitative results were obtained with the LFA technique followed by the sandwich assay. On the other hand, the portion of the nitrocellulose (NC) membrane, where the antigen-antibody complex is already formed in the test area of the LFA test strips, was subsequently used to confirm the electrochemical quantification. The effectiveness of electrochemical quantification was dependent on the presence of electron transfer agents at the electrode surface [20]. Electro-chemical studies were carried out for the reliability of the test results and signal intensity [21-23]. Signal detection of redox species curving in the LFA-modified strip indicates the possibility of developing a one-step analysis format with electrochemical quantification. In numerous published papers, it has been shown that as the concentration of analyte increases, the redox peak current of an electron transfer agent decreases due to the slowing of electron transmission between the paper strip and electrolytic solution. These results confirmed the accuracy of the currently presented cyclic voltammetry (CV) studies. From observing CV curves, it was found that the pattern of oxidation currents reduces with increasing concentration and proved that the responses are concentration-dependent [24-27]. Here, the LFA strip test results are validated by the quantitative and qualitative determination of PCT. The purpose of this study is to detect PCT on a paper strip using LFA and electrochemical CV technique. This new paper strip is a convenient method for quantifying PCT with high sensitivity and low detection limit. This study showed that electrochemical detection is independent of AuNP-antibody conjugation and works normally when colorimetric detection suggests a false positive test, whereas LFA can respond to AuNP-antibody conjugation and antigen-antibody interaction.

Experimental

Reagents and instruments

Chloroauric acid, tri-sodium citrate dihydrate, bovine albumin serum (BSA), disodium hydrogen phosphate, and monobasic sodium phosphate were purchased from CDH Chemicals. Sodium

borohydride and Tween-20 were purchased from Thomas Baker (Chemicals), sucrose, tris (hydroxy-methyl) methylamine, sodium chloride and sodium azide from Fisher Scientific, while mAb and pAb were purchased from mybiosource.com. Glass fiber sample pad (24×260 mm), polyester conjugation pad (70×260 mm), NC membrane (50×260 mm) and absorption pad (21×260 mm) were purchased from Advanced micro devices (mdi) membrane. The electrochemical characterization has been conducted on an Autolab PGSTAT204 potentiostat/galvanostat (Eco Chemie, The Netherlands) using a three-electrode system with the paper strip as working electrode, Ag/AgCl as reference electrode and platinum foil as a counter electrode, in $^-$0.1 M KCl containing 10 mM [Fe(CN)$_6$]$^{3-/4-}$.

Preparation of AuNP-antibody conjugate

AuNP were synthesized by the citrate method. For the synthesis, 50 ml of the aqueous solution of (2.5 mM) hydrogen tetrachloroaurate(III) trihydrate (HAuCl$_4$· xH$_2$O) was prepared and boiled at about 65 °C, and after that 1ml of 5 % aqueous solution of trisodium citrate (TSC; 1 mL) [28-31] was mixed dropwise. The solution was stirred continuously for 30 minutes, resulting in a color variation from pale yellow/colorless to purple and finally to ruby red (Figure 1). For the conjugation of AuNP with pAb, a purified concentration of 0.2 mg ml^{-1} pAb was diluted in PBS buffer (100 mM, pH 7.4). Potassium carbonate is used to maintain pH to 6.7 with a solution of colloidal gold and diluted antibodies. The diluted solution was incubated for 30 minutes at 25 °C followed by the addition of 0.25 % blocking agent BSA and then continued to stir for twenty minutes. Subsequently defining the sanctified concentration of binding pAb, the AuNP-pAb was prepared. For the prediction of conjugation of AuNP-pAb, the absorption peak was monitored at about 523-526 nm by ultraviolet-visible (UV-Vis) spectroscopy. About 15-20 minutes, the entire solution was centrifuged at 8000 rpm. After centrifugation, the unconjugated antibody supernatant was gradually removed. Pallets were resuspended in buffers 10 mmol PBS, 0.5 % BSA, 5 % sucrose, and 0.1 % freshly prepared solution of sodium azide and stored at 4 °C for future use.
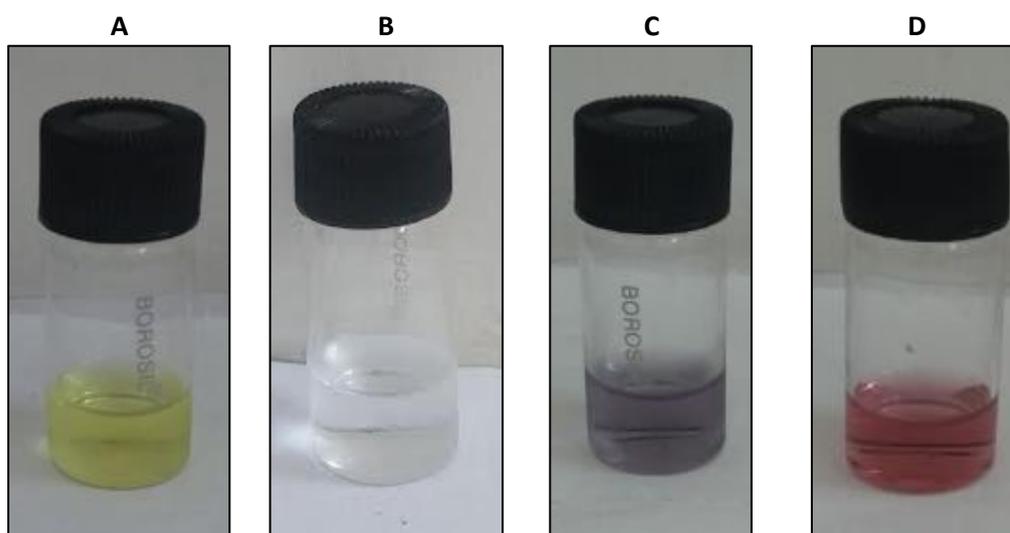

Figure 1. *The appearance of the color of AuNP: (A) 25 mM of HAuCl$_4$·xH$_2$O solution; (B),(C) after adding TSC and continued to stir; (D) ruby red color of prepared AuNP*

Assembling of LFA strip components

The complete assembly parameters of the LFA test are described in Figure 2. The NC membrane has an adhesive plastic backing plate. The conjugate pad (1.4×0.5 cm^2) was pasted in a position overlapping the NC (2.4×0.5 cm^2) membrane by 5 mm. An absorbent pad (2.4×0.5 cm^2) was overlapped on the other side of the membrane by 5 mm. The sample pad (1.3×0.5 cm^2) was further

pasted over the conjugate pad with overlapping of 5 mm length. To confirm the proper placement and operation of the components, the liquid sample was dripped from the sample pad to the absorbent pad. For the preparation of the test line, 0.2 mg ml^{-1} mAb antibody containing PBS was dropped by a micropipette on the NC membrane and dried for 24 h at room temperature. Once fully assembled, LFA strips were stored in a dry place.
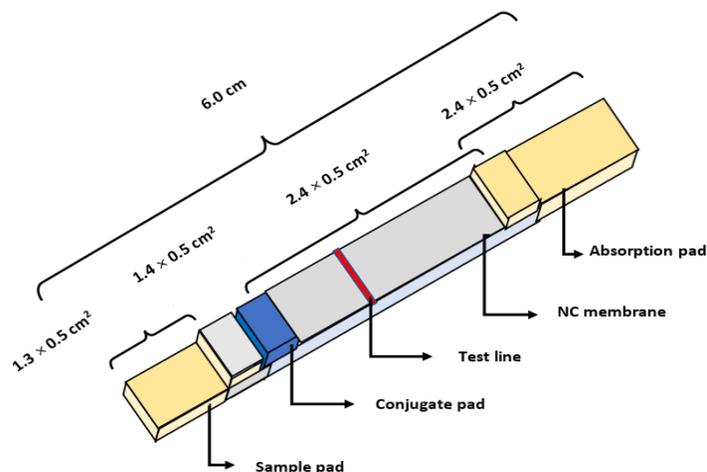

Figure 2. Schematic illustration of LFA test strip

Pre-treatment of pads

The glass fiber sample pad strips were pretreated with an aqueous solution containing 1 % sucrose, 1 % BSA, 0.05 % sodium azide, 20 mol l^{-1} sodium borate, and 0.05 % Tween-20 for 60 min. The strips were dried at 45 °C and stored in a dry state for further use. The polyester fiber conjugation pad was immersed in a solution containing 5 % sucrose and 0.05 % sodium azide in water for 90 minutes and then dried for 120 minutes at 50 °C. The conjugation pad was dipped in 5 ml of pre-prepared conjugate (pAb-AuNP) solution for 24 h. The conjugation pad was then dried at 37 °C and stored for further use. The NC membrane was pretreated by 1 % Tween-20 and 1 % BSA for 1 h and dried at 38 °C for 60 minutes and stored in the dry state for further use.

Results and discussion

In this study, we discussed the qualitative and quantitative determination of the BI-specific biomarker PCT because PCT is promising and very sensitive to increased BI levels and is often reported to be more significant than other biomarkers. PCT ranges from 2 to 10 ng ml^{-1} in sepsis, whereas PCT above 10 ng ml^{-1} indicates a state of septic shock. However, PCT concentration of 2 to 0.15 ng/ml indicates uncertainty in the presence of BI. AuNP is used as a labelling agent and PCT-specific mAb was dropped at the test line by a micropipette. When the complex (AuNP-pAb/PCT) moves through the NC membrane and reaches the test line containing mAb, a sandwich complex (AuNP-pAb /mAb/PCT) is formed. The formation of this complex can be visualized by appearing a red-colored band on the test line due to the presence of AuNP in the sandwich complex. The strength of the red color band indicates PCT concentration which has further been quantified using colorimetric and electrochemical techniques.

Characterization of AuNP and pAb-AuNP conjugate

UV-Vis spectroscopy, transmission electron microscopy (TEM), and scanning electron microscopy (SEM) were used for the spectroscopic and morphological characterization of AuNP and its conjugates. UV-Vis spectroscopy can be used to determine the stability of nanoparticle solution over time. When

AuNP are exposed, they appear in a red solution, but when the particles are conjugated, the solution color turns blue/purple and may turn into a clear solution with a black precipitate. Figure 3 shows the UV-visible absorption spectra of AuNP and its conjugate with pAb. In this graph, the red color curve shows bare AuNP, and a black colour curve is indicates for AuNP-pAb conjugation. Bare AuNP peak was recorded at 524 nm, which approves the existence of sphere-shaped AuNP with remarkable colloidal constancy and consistency in size and composition. The peak of AuNP-pAb was recorded at 530 nm, which explains that AuNP-pAb conjugation is taking place. Here, the shift of the peak to the right indicates a longer wavelength with increasing AuNP [32].

Figure 3. *UV-Vis absorption spectra of AuNP and AuNP-pAb*

For TEM studies, carbon-coated copper grids were used. The prepared AuNP solution (10 µl) was dropped on-grid and dried for 24 h. Experimental data was collected at 200.0 kV and 50000× magnification. The TEM images reveal that synthesized AuNPs are well separated and spherical (Figure 4A), indicating their stable dispersion in the solution condition. Furthermore, the synthesized particles are monodispersed, having a size range from 15.4 -25.6 nm (Figure 4B).

Figure 4. *TEM images of AuNP*

For the preparation of SEM samples, the drop-casting method was applied. By this method, polyvinyl alcohol and AuNP (PVA-AuNP) film were prepared. In this method, the ITO plate surface (1.0×1.0 cm^2)

was ultrasonically cleaned with an aqueous solution of ammonia and ethyl alcohol. The mixed solution (1ml of colloid gold and 5 % PVA) was dropped on the bare surface of ITO. Then the strips were dried at 140 °C for 1.5 h to make PVA-AuNP film [33]. After that, the annealing process of PVA-AuNP film was done and kept about 4-5 h at different temperatures (400-600 °C). Eventually, the strengthened film was cooled at room temperature in the air. The SEM image of the sample has been demonstrated in Figure 5. Experimental data was collected at 20.00 kV and x 1000 magnification.
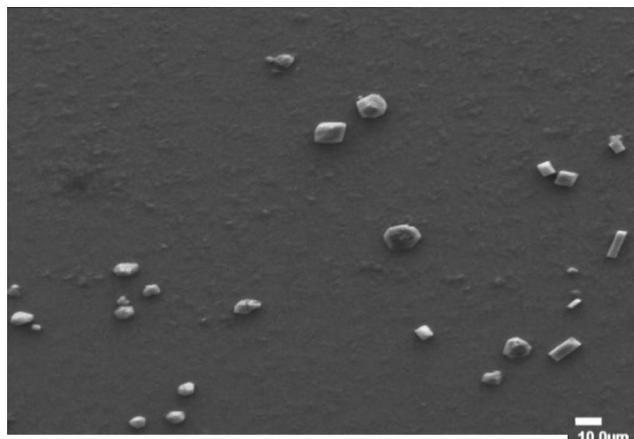
Figure 5. *SEM image of AuNP deposited on ITO glass after annealing at 400 °C*

Optimization of standard sample assay

For the LFA reaction, a sandwich analysis was performed to detect the PCT signal. For this purpose, standard solutions of PCT with concentrations of 1, 2, 10, 20, 30, 40, 50, and 60 ng ml^{-1} were prepared from the stock solution of 0.1 mg ml^{-1} solution in PBS solution (pH 7.4). The sample pad and conjugate pad were pretreated with buffers and used to develop antigen-antibody interaction. The AuNP-pAb complex was applied to the conjugation pad. Samples containing PCT antigen with different standard concentrations were dropped to the sample pad to initiate the reaction. The sample antigen interacts with the pAb-AuNP complex and forms a labeled antigen-antibody complex as it starts flowing through the sample pad. This complex moves across a porous membrane where specific mAb is already present in the test zone, forming a sandwich complex. The test line was drawn on the NC membrane 2.1 cm away from the conjugated pad. When PCT (100 µl) was dropped at sample pad at concentrations of 10 to 60 ng ml^{-1}, a strong red band appeared at the test line (Figure 6d-i).
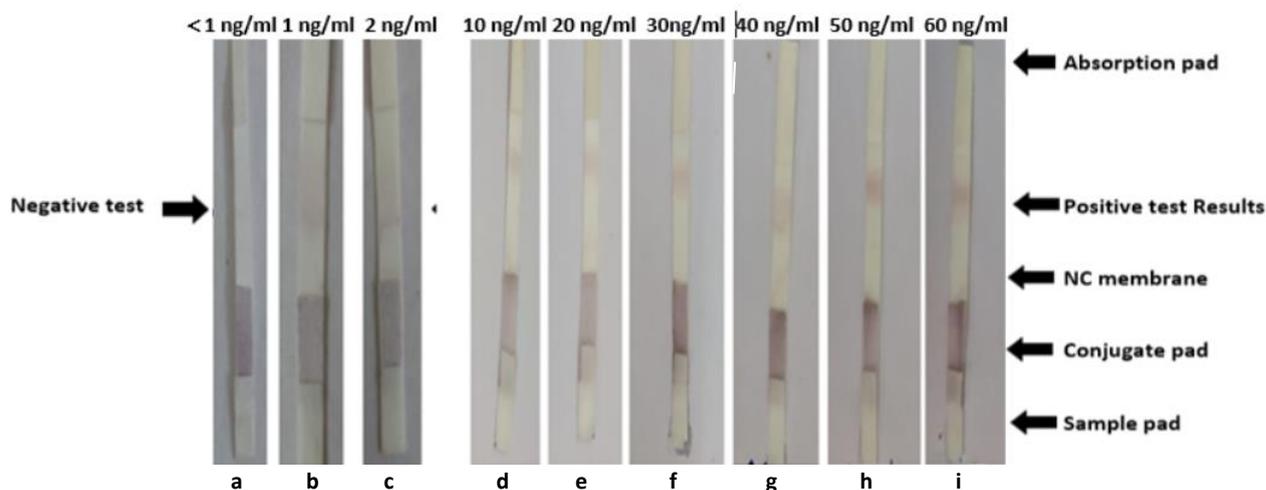

Figure 6. *Illustration of LFA strips test results of different concentrations of PCT: (a) <1 ng ml^{-1} and (b) 1 ng ml^{-1} are showing negative test results; (c) 2 ng ml^{-1} is showing weak positive bands; (d-i) 10 to 60 ng ml^{-1} are showing strong positive test results*

At the concentration of 2 ng ml^{-1}, a weak red band appeared at the test line (Figure 6c), and thus, this concentration has been considered as the qualitative limit of detection of the test assay. However, at 1 ng ml^{-1} (Figure 6b) and lower concentrations (Figure 6a) no bands appeared at the test line, and thus, 1 ng ml^{-1} has been considered as a negative test result.

Electrochemical characterization of LFA strip and response studies

Cyclic voltammetry (CV) studies were conducted for electrochemical detection of a range of PCT concentrations using an Autolab potentiostat/galvanostat instrument with a three-electrode setup. Platinum wire was used as the counter electrode, Ag/AgCl as the reference electrode, and the portion of NC membrane cut from the modified LFA test strip (pAb-AuNP/mAb/PCT) was used as the working electrode (paper strip). For electrochemical analysis, 0.1 M KCl containing 10 mM [Fe(CN)$_6$]$^{3-/4-}$ solution was used as a redox probe [19,35]. In the present work, CVs were performed with the paper strip as a working electrode which exhibits low conductivity. Thus, to enhance electron transmission between the working electrode and electrolyte and to record oxidation/reduction currents in CV curves, the redox probe [Fe(CN)$_6$]$^{3-/4-}$ was added as a marker to investigate changes in electrode behaviour after loading different concentrations of PCT on the paper strip [34,36,37].

To obtain voltammetric signals, portions of the NC (2.4×0.5 cm^2) membrane of the strips which have an antigen-antibody complex, were cut (2 cm) and immersed in a redox probe solution (0.1 M KCl containing 10 mM [Fe(CN)$_6$]$^{3-/4-}$. CVs were performed between -0.4 and 0.8 V at the scan rate of 50 mV s^{-1}. Figure 7A shows decreasing oxidation/reduction currents in recorded CVs for every increase in the concentration of PCT analyte on the paper strip. In an electrochemical investigation through CV, redox currents produced as a result of electron transfer from an electrolyte to a working electrode or *vice versa* were monitored. The intensity of produced redox currents depends upon the electroactive species present in the electrolytic solution. With the help of this mechanism, redox currents are observed to identify the PCT analyte on the paper strip. Oxidation and reduction current peaks are not visible in recorded CVs in our work as the paper strip is a poor conductor and does not facilitate charge transfer. Thus, a characteristic cyclic voltammogram is not obtained even after the application of redox agents. Nevertheless, the recorded CVs of the paper strips in the presence of redox agents in the solution are in conformity with work published by various research groups [38,39]. Thus, to study variation in oxidation current of the strip with respect to varying PCT concentrations, the oxidation CV signal has been recorded at the fixed potential (0.3V). When the concentration of 1 ng ml^{-1} PCT paper strip was investigated by CV, the oxidation current was 60.03 μA, and when the concentration of the analyte was increased to 2 ng ml^{-1}, a decrease of oxidation current to 53.29 μA was observed. On further increasing of the analyte concentration from 10, 20, 30, 40, 50 and 60 ng ml^{-1}, a continuous decrease of oxidation current was observed as 46.96, 37.21, 29.52, 23.49, 21.13 and 17.46 μA, respectively. This can be attributed to higher loading of PCT on the paper strip surface with increasing concentration, which hinders electron transmission between the redox probe and the electrode, and so, the current density is decreased. Using CV current responses, the calibration curve is obtained and presented in Figure 7B as a function of measured oxidation current at 0.3 V and PCT concentration on the paper strip in the range of 1 to 60 ng ml^{-1}. Linear proportionality of this plot indicates that magnitude of current changes linearly with the change in analyte concentration, while the negative slope of this plot indicates that oxidation current decreases with the increase of analyte on the paper strip. The linear proportionality of the current value and PCT concentration in the range from 1 to 60 ng ml^{-1} corresponds to the equation (1), showing the regression coefficient value of 0.97 and sensitivity value of 0.695 μA ml ng^{-1}.

$$I = 0.695\,[C_{PCT}] + 54.646 \tag{1}$$

A   **B**

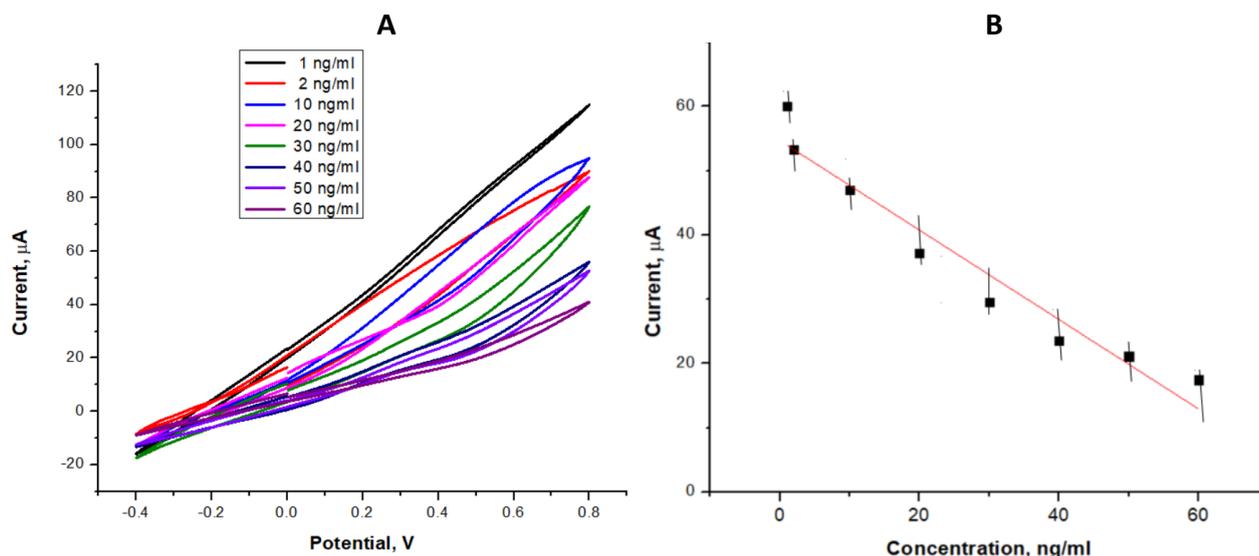***Figure 7.*** *(A) CV recorded for modified LFA strip as a function of PCT concentrations (1 - 60 ng ml^{-1}) in 0.1 M KCl containing 10 mM [Fe(CN)$_6$]$^{3-/4-}$; (B) calibration plot of oxidation current at 0.3 V as a function of PCT concentration*

Conclusions

The present paper successfully developed a portable and inexpensive detection test kit for the quantitative and qualitative detection of PCT analyte through LFA and electrochemical CV techniques. Here, AuNP performed excellent specificity and color appearance at the test line. The color intensity on the test zone was directly proportional to the concentration of the PCT analyte. LOD of the LFA technique of 2 ng ml^{-1} was found qualitatively and 1 ng ml^{-1} quantitatively. By electrochemical CV response studies, a linear relation between oxidation current and PCT in the concentration range of 1 to 60 ng ml^{-1} was obtained, with the sensitivity of the modified LFA strip of 0.695 µA ml ng^{-1}. This approach proves that for electrochemical detection of PCT, there is no need to use highly conductive substrates such as gold, silver, ITO, and expensive quantitative equipment. Hence, LFA and electrochemical techniques are convenient and easy POC techniques to detect BI-specific biomarker PCT.

References

[1] Y. Gupta, A.S. Ghrera, *Archives of Microbiology* **203** (2021) 3767-3784. https://doi.org/10.1007/s00203-021-02357-9

[2] L.-M. Lei, J.-S. Wu, N.-Q. Gan, L. R. Song, *Clinica Chimica Acta* **348(1-2)** (2004) 177-180. https://doi.org/10.1016/j.cccn.2004.05.019

[3] T. Yu, S. Gao, A. Yin, Y. Tang, Y. Wu, L. Li, M. Li, *Journal of Immunoassay and Immunochemistry* **34(4)** (2013) 365-375. https://doi.org/10.1080/15321819.2012.744999

[4] L. Cinquanta, D.E. Fontana, N. Bizzaro, *Autoimmunity Highlights* **8(1)** (2017) 9. https://doi.org/10.1007/s13317-017-0097-2

[5] R. Gautam, K. Parajuli, T. Tshokey, J. Stenos, J. B. Sherchand, *BMC Infectious Diseases* **20** (2020) 138. https://doi.org/10.1186/s12879-020-4861-y

[6] S. Sharma, J. Zapatero-Rodríguez, P. Estrela, R. O'Kennedy, *Biosensors (Basel)* **5(3)** (2015) 577-601. https://doi.org/10.3390/bios5030577

[7] B. N. Khlebtsov, R. S. Tumskiy, A. M. Burov, T. E. Pylaev, N. G. Khlebtsov, *ACS Applied Nano Materials* **2(8)** (2019) 5020-5028. https://doi.org/10.1021/acsanm.9b00956

[8] M. Sajid, A.-N. Kawde, M. Daud, *Journal of Saudi Chemical Society* **19(6)** (2015) 689-705. https://doi.org/10.1016/j.jscs.2014.09.001

[9] K. M. Koczula, A. Gallotta, *Essays in Biochemistry* **60(1)** (2016) 111-120. https://doi.org/10.1042/EBC20150012

[10] X.-Y. Shao, C.-R. Wang, C.-M. Xie, X.-G. Wang, R.-L. Liang, W.-W. Xu, *Sensors (Basel)* **17(3)** (2017) 480. https://doi.org/10.3390/s17030480

[11] N. Zhan, Y. Zhou, L. Mei, Y. Han, H. Zhang, *Analytical Sciences* **35(3)** (2019)257-263. https://doi.org/10.2116/analsci.18p357

[12] A. L. Vijayan, Vanimaya, S. Ravindran, R. Saikant, S. Lakshmi, R. Kartik, Manoj. G. *Journal of Intensive Care* **51** (2017) 5. https://doi.org/10.1186/s40560-017-0246-8

[13] P. Schuetz, W. Albrich, B. Mueller, *BMC Medicine* **9** (2011) 107. https://doi.org/10.1186/1741-7015-9-107

[14] A. Hohn, S. Schroeder, A. Gehrt, K. Bernhardt, B. Bein, K. Wegscheider, M. Hochreiter, *BMC Infectious Diseases* **13** (2013) 158. https://doi.org/10.1186/1471-2334-13-158

[15] I. Samsudin, S. D. Vasikaran, *The Clinical Biochemist Reviews* **38(2)** (2017) 59-68. https://pubmed.ncbi.nlm.nih.gov/29332972

[16] K. V. Serebrennikova, J. V. Samsonova, A. P. Osipov, *Microchimica Acta* **186(7)** (2019) 423. https://doi.org/10.1007/s00604-019-3550-2

[17] K. Serebrennikova, J. Samsonova, A. Osipov, *Nano-Micro Letters* **10(2)** (2018) 24. https://doi.org/10.1007/s40820-017-0180-2

[18] K. V. Serebrennikova, J. V. Samsonova, A. P. Osipov, *Moscow University Chemistry Bulletin* **73(3)** (2018) 131-134. https://doi.org/10.3103/S0027131418030070

[19] A. Sharma Ghrera, *Analytica Chimica Acta* **1056** (2019) 26-33. https://doi.org/10.1016/j.aca.2018.12.047

[20] C. M. Pandey, A. Sharma, G. Sumana, I. Tiwari, B. D. Malhotra, *Nanoscale* **5(9)** (2013) 3800-3807. https://doi.org/10.1039/C3NR34355C

[21] A. S. Ghrera, M. K. Pandey, B. D. Malhotra, *Biosensors and Bioelectronics* **80** (2016) 477-482. https://doi.org/10.1016/j.bios.2016.02.013

[22] A. S. Ghrera, C. M. Pandey, Md. A. Ali, B. D. Malhotra, *Applied Physics Letters* **106(19)** (2015) 193703. https://doi.org/10.1063/1.4921203

[23] A. Sharma, C. M. Pandey, G. Sumana, U. Soni, S. Sapra, A. K. Srivastava, T. Chatterjee, B. D. Malhotra, *Biosensors and Bioelectronics* **38(1**) (2012) 107-113. https://doi.org/10.1016/j.bios.2012.05.010

[24] K. Ionue, P. Ferrante, Y. Hirano, T. Yasukawa, H. Shiku, T. Matsue, *Talanta* **73(5)** (2007) 886-892. https://doi.org/10.1016/j.talanta.2007.05.008

[25] Y. Huang, P. Kannan, L. Zhang, T. Chen, D.-H. Kim, *RSC Advances* **5(72)** (2015) 58478-58484. https://doi.org/10.1039/C5RA10990F

[26] W. Iwasaki, C. Kataoka, K. Sawadaishi, K. Suyama, N. Morita, M. Miyazaki, *Sensors* **20(17)** (2020) 4781. https://doi.org/10.3390/s20174781

[27] X. Zhu, P. Shah, S. Stoff, H. Liu, C.-Y. Li, *Analyst* **139(11)** (2014) 2850-2857. https://doi.org/10.1039/C4AN00313F

[28] J. Turkevich, P.C. Stevenson, J. Hillier, *Disscussions of the Faraday Society* **11** (1951) 55-75. https://doi.org/10.1039/DF9511100055

[29] J. Dong, P. L. Carpinone, G. Pyrgiotakis, P. Demokritou, B. M. Moudgil, *Kona Powder and Particle Journal* **37** (2020) 224-232. https://dx.doi.org/10.14356 %2Fkona.2020011

[30] P. Suchomel, L. Kvitek, R. Prucek, A. Panacek, A. Halder, S. Vajda, R. Zboril, *Scientific Reports* **8(1)** (2018) 4589. https://doi.org/10.1038/s41598-018-22976-5

[31] F. F. M. AL-Kazazz, K. A. F. AL-Imarah, I. A. Al-Hasnawi, L. Agelmashotjafar, B. A. Abdul-Majeed, *International Journal* of *Engineering Research an*d *Applications* **3(6)** *(*2013) 21-30.

[32] V. D. Pham, H. Hoang, T. H. Phan, U. Conrad, H. H. Chu, *Advances in Natural Sciences: Nanoscience and Nanotechnology* **3(4)** (2012) 045017. http://dx.doi.org/10.1088/2043-6262/3/4/045017

[33] T. Feng, L. Ding, L. Chen, J. Di, *Journal* of *Experimental Nanoscience* **14(1)** (2019) 13-22. https://doi.org/10.1080/17458080.2018.1520399

[34] W. A. Ameku, W. R. de Araujo, C. J. Rangel, R. A. Ando, Thiago R. L. C. Paixão, *ACS Applied Nano Materials* **2(9)** (2019) 5460-5468. https://doi.org/10.1021/acsanm.9b01057

[35] A. Sharma, Z. Matharu, G. Sumana, P. R. Solanki, C. G. Kim, B. D. Malhotra, *Thin Solid Films* **519(3)** (2010) 1213-1218. https://doi.org/10.1016/j.tsf.2010.08.071

[36] X. Li, C. Zhao, X. Liu, *Microsystems & Nanoengineering* **1** (2015) 15014. https://doi.org/10.1038/micronano.2015.14

[37] S. Kumar, S. Kumar, C.M. Pandey, B.D. Malhotra, *Journal of Physics: Conference Series* **704** (2016) 012010. https://doi.org/10.1088/1742-6596/704/1/012010

[38] L. C. Shriver-Lake, D. Zabetakis, W. J. Dressick, D. A. Stenger, S. A. Trammell, *Sensors* **18(2)** (2018) 328. https://dx.doi.org/10.3390%2Fs18020328

[39] S. A. Trammell, L. C. Shriver-Lake, W. J. Dressick, *Sensors and Actuators B* **239** (2017) 951-961. https://doi.org/10.1016/j.snb.2016.08.087